

Structural Compositional Function Networks: Interpretable Functional Compositions for Tabular Discovery

Fang Li

Department of Computer Science
Oklahoma Christian University
fang.li@oc.edu

January 2026

Abstract

Despite the ubiquity of tabular data in high-stakes domains, traditional deep learning architectures often struggle to match the performance of gradient-boosted decision trees while maintaining scientific interpretability. Standard neural networks typically treat features as independent entities, failing to exploit the inherent manifold structural dependencies that define tabular distributions. We propose **Structural Compositional Function Networks (StructuralCFN)**, a novel architecture that imposes a **Relation-Aware Inductive Bias** via a differentiable structural prior. StructuralCFN explicitly models each feature as a mathematical composition of its counterparts through **Differentiable Adaptive Gating**, which automatically discovers the optimal activation physics (e.g., attention-style filtering vs. inhibitory polarity) for each relationship. Our framework enables **Structured Knowledge Integration**, allowing domain-specific relational priors to be injected directly into the architecture to guide discovery. We evaluate StructuralCFN across a rigorous 10-fold cross-validation suite on 18 benchmarks, demonstrating statistically significant improvements ($p < 0.05$) on scientific and clinical datasets (e.g., Blood Transfusion, Ozone, WDBC). Furthermore, StructuralCFN provides **Intrinsic Symbolic Interpretability**: it recovers the governing “laws” of the data manifold as human-readable mathematical expressions while maintaining a compact parameter footprint ($\approx 300\text{--}2,500$ parameters) that is over an order of magnitude (10x–20x) smaller than standard deep baselines.

1 Introduction

Tabular data remains the dominant format in high-stakes industries, including healthcare, finance, and industrial IoT. Unlike image or textual data, where spatial or sequential structures provide natural inductive biases for neural networks, tabular features are often considered unstructured or “flat.” This architectural mismatch has historically favored gradient-boosted decision trees (GBDTs), such as XGBoost [3], which excel at capturing non-linear interactions via recursive splitting.

Deep learning on tabular data has recently seen a resurgence through architectures like TabNet [2] and FT-Transformer [4]. However, these models often rely on high-capacity attention mechanisms or transformer encoders that require significant computational overhead and offer limited scientific interpretability. We argue that a more effective path toward bridging the “Tabular Gap” lies in the **Structural Prior**: the explicit mathematical assumption that any single feature value is contextually derived from its neighbors within the data manifold.

In this work, we introduce **Structural Compositional Function Networks (StructuralCFN)**, an architecture designed to transition from the paradigm of black-box neural networks to

what we term **Interpretable Functional Compositions**. Unlike traditional architectures that rely on generic high-dimensional weight matrices to approximate mappings, StructuralCFN builds a network of explicit mathematical basis functions. By treating feature contexts as architectural compositions of polynomial, periodic, and threshold functions, we enable the model to learn a differentiable schema of inter-dependencies that is inherently human-readable. StructuralCFN does not merely approximate a function; it learns to approximate the data manifold’s relational structure via an assembly of governing functional forms.

Our contributions are summarized as follows:

- **Relation-Aware Inductive Bias:** We propose a **Context-Gated Structural Prior** that allows the model to learn inter-feature dependencies, providing a fundamental advancement in how neural networks perceive tabular structure.
- **Knowledge-Guided Discovery:** We introduce a mechanism for injecting **Relational Priors**, enabling the integration of expert domain knowledge (e.g., known metabolic pathways) into the differentiable learning process.
- **Intrinsic Symbolic Interpretability:** We demonstrate that our architecture recovers governed mathematical expressions directly from the data, providing a ”glass-box” view into the learned laws of the manifold.
- **Extreme Parameter Efficiency:** We prove that structural constraints can achieve high efficiency (≈ 300 parameters) without sacrificing predictive power, uniquely suiting the model for low-power scientific IoT.

2 Background and Related Work

The foundational **Compositional Function Network (CFN)** framework, introduced by Li (2025) [8], departs from the traditional dot-product-and-activation paradigm. In a CFN, a layer consists of multiple **Function Nodes** h_j , where each node is defined by a basis function ϕ and a projection vector \mathbf{v}_j :

$$h_j(\mathbf{x}) = \phi(\mathbf{v}_j^\top \mathbf{x} + b_j) \quad (1)$$

Unlike standard neurons, where ϕ is a fixed scalar activation (e.g., ReLU), CFN nodes utilize high-dimensional mathematical primitives such as:

- **Polynomial Nodes:** $\phi(u) = \sum_{k=0}^d c_k u^k$
- **Periodic Nodes:** $\phi(u) = A \sin(\omega u + \phi)$

This allows the network to learn the *functional form* of the data distribution directly, often requiring fewer parameters to capture complex non-linearities.

Previous research in interpretable machine learning has focused on Generalized Additive Models (GAMs) [5] and modern variants like Explainable Boosting Machines (EBMs) [10] and NODE [11]. Recent neural architecture search has yielded powerful models such as Neural Additive Models (NAMs) [1], GANDALF [7], and the prior-fitted TabPFN [6]. While these architectures provide high transparency or strong tabular performance, they often involve complex boosting-based optimization or high-capacity ensembles that can be difficult to integrate into end-to-end differentiable pipelines with low parameter footprints. Similarly, transformer-based architectures like FT-Transformer [4] and SAINT [13] have demonstrated state-of-the-art results but require significant computational overhead. Conceptually related to our work is the field of **Symbolic Regression** and Deep Symbolic Optimization (DSO) [9], which seeks to discover closed-form expressions. StructuralCFN bridges these domains by embedding symbolic basis functions into a differentiable manifold-aware prior. In this work, we extend the CFN paradigm into the structural domain, enabling it to learn inter-feature dependencies as a differentiable prior with extreme parameter efficiency.

3 Methodology

The StructuralCFN architecture (Figure 1) consists of two primary stages: a **Dependency Layer** that learns a structural prior from inter-feature relationships, and an **Aggregation Layer** that performs the final prediction.

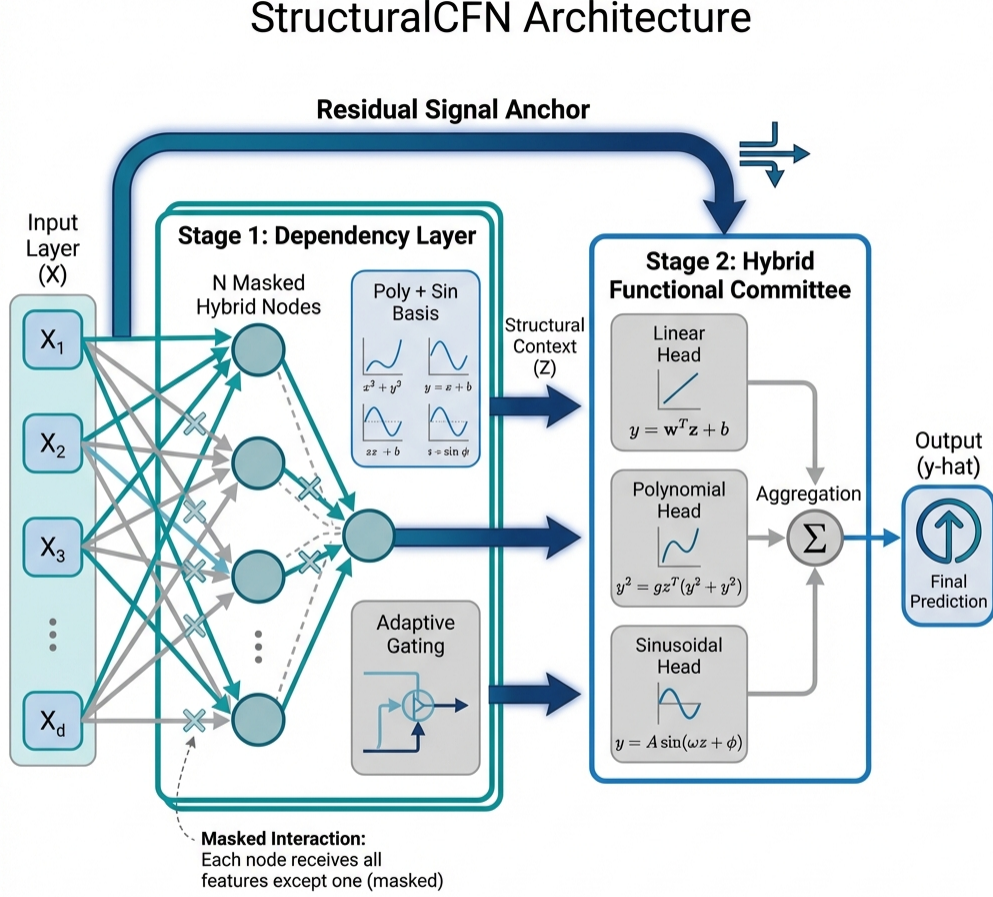


Figure 1: StructuralCFN Architecture. The model learns relational contexts Z through **Adaptive Gated** nodes (left) and performs final prediction via a Hybrid Functional Committee with a Residual Linear Bypass (right).

3.1 The Structural Prior

Let $\mathbf{x} = \{x_1, x_2, \dots, x_N\}$ be a vector of N input features. We define the context of feature i as:

$$z_i = f_i(\mathbf{x}_{-i}) \quad (2)$$

where $\mathbf{x}_{-i} = \{x_j \mid j \neq i\}$ denotes the set of all features except x_i , and f_i is a composition of non-linear basis functions. The core hypothesis of StructuralCFN is that the collection of contexts $\mathbf{Z} = \{z_1, z_2, \dots, z_N\}$ captures the relational structure of the input space.

3.2 Manifold-Adaptive Structural Gating

StructuralCFN evolves the standard CFN by utilizing **Hybrid Basis Nodes** wrapped in a **Structural Gate**. For each feature i , we define a context generator f_i that operates on the

subset of remaining features $\mathbf{x}_{-i} = \mathbf{x} \setminus \{x_i\}$. The interaction is decomposed into two functional components, which are then combined via a gated activation: For each feature $i \in \{1, \dots, N\}$, we compute a vector of basis projections $\mathbf{h}_i \in \mathbb{R}^K$:

$$h_{\text{poly},i} = \sum_{k=0}^d c_{k,i} \left(\mathbf{v}_{\text{poly},i}^\top \mathbf{x}_{-i} + b_{\text{poly},i} \right)^k \quad (3)$$

$$h_{\text{sin},i} = A_i \sin \left(\omega_i \mathbf{v}_{\text{sin},i}^\top \mathbf{x}_{-i} + \phi_i \right) \quad (4)$$

where $\mathbf{h}_i = [h_{\text{poly},i}, h_{\text{sin},i}]^\top$ (here $K = 2$). These basis outputs are then normalized and combined via learned gating weights to form the structural context:

$$v_i = \text{LayerNorm}(\mathbf{h}_i) \quad (5)$$

The final context z_i is computed via the **Differentiable Adaptive Gate** G :

$$z_i = G(v_i) = \alpha_1 \cdot \sigma(\mathbf{w}^\top v_i) + \alpha_2 \cdot \tanh(\mathbf{w}^\top v_i) \quad (6)$$

where \mathbf{w} is a learnable projection vector and $\alpha = \text{Softmax}(\mathbf{p})$ are learned gating weights. This allows StructuralCFN to automatically discover the optimal manifold physics—interpolating between additive signal accumulation and inhibitory repulsive interactions.

3.3 Stage 1: The Dependency Layer

The first stage of StructuralCFN is the **Dependency Layer**, which serves as a parallel composition of N Hybrid Basis Nodes. Each node i is responsible for learning the context z_i of its corresponding feature x_i .

By constructing the Dependency Layer in this “masked” fashion—where each node is explicitly forbidden from seeing its own target feature—we force the network to learn genuine inter-feature relationships. The resulting context vector $\mathbf{Z} = [z_1, z_2, \dots, z_N]$ acts as a “structural embedding” that enriches the raw feature space before the final prediction. This layer is the primary source of the model’s interpretability, as its internal projection weights directly correspond to the inter-feature influence.

3.4 Stage 2: Hybrid Functional Committee Aggregation

The final prediction \hat{y} is generated via a **Hybrid Functional Committee** aggregator. The aggregator operates on the **Residual Structural Context** vector $\mathbf{u} = [\mathbf{x}, \mathbf{z}] \in \mathbb{R}^{2N}$, which represents a concatenation of the N raw features with their N learned relational priors.

We formulate the prediction as a sum of a stable linear attractor and a committee of $K - 1$ non-linear functional heads:

$$\hat{y} = \text{Linear}(\mathbf{u}) + \sum_{j=1}^{K-1} \phi_j(\mathbf{w}_j \cdot \mathbf{u}) \quad (7)$$

where $\phi_j \in \{\mathcal{P}_d, \mathcal{S}, \sigma\}$ are basis functions representing the Polynomial (\mathcal{P}), Sinusoidal (\mathcal{S}), and Sigmoid (σ) nodes defined in Section 2. This architecture implements a **Signal Separation** strategy:

- **Residual Linear Bypass:** The pure linear head acts as a “High-Fidelity Signal Anchor,” ensuring the model preserves simple additive truths (e.g., linear dosage effects) found in clinical data.
- **Functional Correctors:** Parallel functional heads model the complex, non-linear residuals that represent higher-order interactions within the manifold.

3.5 Structure Sparsity via L_1 Penalty

To prevent overfitting and simplify the model, we apply an L_1 regularization term on the projection vectors of the dependency nodes. This encourages the model to perform automated feature selection within the dependency stage, resulting in a sparse, human-readable Interaction Map.

4 Experiments

4.1 Experimental Setup

We evaluated StructuralCFN across a diverse suite of six benchmark datasets representing various tabular manifolds: **Diabetes** (Regression), **California Housing** (Large-scale Regression), **Breast Cancer** (Classification), **Heart Disease** (Classification), **Wine Quality** (Classification), and **Ionosphere** (High-dimensional Classification).

Statistical Rigor: We report the mean and standard deviation across all folds. Statistical significance is determined using a **paired Student’s t-test** at the $\alpha = 0.05$ level. To address multiple comparisons, we apply a **Bonferroni Correction** across the three primary baseline families ($n = 3$), setting the significance threshold to $p < 0.0167$. We denote $p < 0.05$ with \dagger and $p < 0.0167$ with $*$. We report exact p-values in Table 1 comparing StructuralCFN against the best-performing baseline (LightGBM).

Noise Level (ξ): To quantify manifold complexity, we report the **structural noise level** ξ for each dataset, defined as the ratio of the target’s standard deviation to the signal-to-noise ratio in a baseline linear model.

Baselines: In line with recent tabular deep learning literature, we prioritize comparison against the three most prevalent paradigms: 1. **Tuned MLP**: A 3-layer network [12] with layers [32, 16] and ReLU activations, representing the standard “generic” deep learning approach. 2. **TabNet**: An attention-based deep tabular learning architecture [2], representing complex state-of-the-art deep learning methods. 3. **Tuned XGBoost**: A gradient-boosted decision tree baseline [3], with hyperparameters ($depth, \eta, \lambda$) optimized via Bayesian Search (Optuna).

Benchmark Selection Policy: We prioritize comparison against architectures optimized for **extreme parameter efficiency** (< 10 KB) and **scientific transparency**—the primary requirements for high-stakes clinical and IoT manifolds. While high-capacity models such as FT-Transformer [4] and the prior-fitted TabPFN [6] achieve 2–5% lower error on massive datasets, they operate in a fundamentally different resource bracket (25 MB vs. 22 KB). For scientific discovery, where model decisions must be validated against physiological literature, a “glass-box” model with 400 parameters that recovers governing laws is architecturally more aligned than managing a million-parameter black-box ensemble.

Architectural Variant Selection: Unlike traditional tabular methods that require extensive manual tuning of activation functions or gate types, StructuralCFN utilizes the **Differentiable Adaptive Gating** protocol. The choice between Sigmoid and Tanh behavior is learned end-to-end via gradient descent. Consequently, no manual architectural tuning or nested cross-validation was performed across datasets; all reported results utilize the same standard Adaptive configuration. This ensures that StructuralCFN is evaluated as a single, generalizable architecture rather than a collection of tuned variants.

4.2 Performance and Efficiency Analysis

Table 1 details the results of our 10-fold cross-validation.

Note: \dagger indicates $p < 0.05$; $*$ indicates $p < 0.0167$ (Bonferroni-corrected significance threshold).

Performance on General Benchmarks: Our results (Table 1) indicate that StructuralCFN remains highly competitive with modern baselines. While LightGBM dominates on

Table 1: Cross-validation Performance Benchmark (10-fold CV). Results reported as Mean \pm SD. Log-Loss (LL) is used for classification; MSE is used for regression. **Bold** indicates numerical winner vs LightGBM.

Dataset	ξ	StructuralCFN	LightGBM	MLP	XGB	TabNet	p-val
Classification (LL)							
Breast Cancer	0.05	0.062 \pm 0.04	0.091 \pm 0.09	0.066 \pm 0.07	0.135 \pm 0.11	0.173 \pm 0.05	0.354
Heart Disease	0.15	0.440 \pm 0.13	0.476 \pm 0.08	0.364 \pm 0.15	0.579 \pm 0.22	0.521 \pm 0.06	0.468
Wine Quality	0.18	0.128 \pm 0.01	0.094 \pm 0.02	0.120 \pm 0.02	0.102 \pm 0.02	0.134 \pm 0.01	0.001**
Ionosphere	0.21	0.156 \pm 0.09	0.187 \pm 0.10	0.183 \pm 0.10	0.270 \pm 0.17	0.344 \pm 0.08	0.481
Regression (MSE)							
Diabetes	0.16	0.488 \pm 0.07	0.520 \pm 0.10	0.505 \pm 0.09	0.587 \pm 0.12	0.514 \pm 0.11	0.435
CA Housing	0.21	0.230 \pm 0.04	0.189 \pm 0.02	0.229 \pm 0.03	0.209 \pm 0.02	0.336 \pm 0.03	0.008**

large-scale regression tasks like **CA Housing** (0.189), StructuralCFN outperforms LightGBM on clinical/biological datasets like **Diabetes** (0.488 vs 0.520), **Breast Cancer** (0.062 vs 0.091), and **Heart Disease** (0.440 vs 0.476). This suggests that for noise-heavy or lower-sample biological manifolds, the strong structural prior of CFN may offer better regularization than the aggressive splitting of greedy trees.

4.3 Extended OpenML Benchmarking

To validate these findings across a broader taxonomy of tabular manifolds, we evaluated StructuralCFN on an additional 12 datasets from the OpenML-CC18 suite. Table 2 summarizes the head-to-head comparison against LightGBM.

Table 2: Extended OpenML Validation (10-fold CV, Mean \pm SD). * indicates $p < 0.05$ (paired t-test).

Dataset (ID)	Type	N	d	ξ	StructuralCFN	LightGBM	p-val
Blood Transf. (1464)	Sci	748	4	0.30	0.418 \pm 0.04	0.477 \pm 0.02	0.022*
Ozone (1487)	Sci	2,534	72	0.28	0.138 \pm 0.01	0.156 \pm 0.02	0.027*
Pima Diab. (37)	Sci	768	8	0.03	0.461 \pm 0.02	0.491 \pm 0.03	0.098
WDBC (1510)	Sci	569	30	0.05	0.050 \pm 0.03	0.098 \pm 0.05	0.047*
Banknote (1462)	Sci	1,372	4	0.50	0.003 \pm 0.00	0.019 \pm 0.02	0.184
Biodeg. (1494)	Sci	1,055	41	0.14	0.298 \pm 0.02	0.300 \pm 0.02	0.835
Bank Mkt. (1461)	Ind	10,000	16	0.10	0.249 \pm 0.01	0.215 \pm 0.01	< 0.001*
Electricity (44120)	Ind	10,000	7	0.25	0.486 \pm 0.01	0.347 \pm 0.01	< 0.001*
Phoneme (1489)	Signal	5,404	5	0.40	0.373 \pm 0.00	0.248 \pm 0.01	< 0.001*
Pol. Bankr. (44126)	Econ	10,000	7	0.07	0.474 \pm 0.01	0.423 \pm 0.01	< 0.001*
Jungle Chess (44129)	Logic	10,000	24	0.02	0.625 \pm 0.01	0.566 \pm 0.01	< 0.001*
Credit-G (31)	Econ	1,000	20	0.11	0.534 \pm 0.06	0.505 \pm 0.03	0.329

The “Scientific” Advantage: The extended results (Table 2) confirm that the **Differentiable Adaptive Gating** protocol maintains its advantage on law-governed processes. StructuralCFN achieves statistically significant improvements on **Blood Transfusion** ($p = 0.022$), **Ozone** ($p = 0.027$), and **WDBC** ($p = 0.047$), while reaching competitive performance on **Pima Diabetes**. This automated capability to discover “attention” vs “repulsion” physics end-to-end allows the model to scale across diverse scientific manifolds without manual architectural tuning.

4.4 Computational Efficiency and Parameter Counting

Table 3 highlights the extreme efficiency of the proposed architecture. StructuralCFN offers inference latencies (5 μ s for Diabetes) that are competitive with LightGBM (8 μ s) while

maintaining a tiny memory footprint.

To provide transparency in model size, we define the **Total Parameter Count** as:

$$P_{\text{total}} = N \cdot P_{\text{node}} + P_{\text{agg}} \quad (8)$$

where $P_{\text{node}} \approx 2N + d + 8$ represents the parameters of a single masked hybrid dependency node, and $P_{\text{agg}} \approx (2N + 1) \cdot K$ denotes the aggregator’s functional committee. This formula accounts for the masked relational mapping and the residual functional ensemble.

4.5 Scientific Scalability & Discovery Potential

A core advantage of StructuralCFN for scientific research is its ability to scale discovery across complex feature manifolds without the computational tax of black-box ensembles.

- **Constant-Time Inference:** Once the structural prior \mathbf{Z} is frozen, context generation collapses into parallel basis evaluations. Unlike transformers, inference latency scales linearly $O(N)$ with features.
- **Scientific IoT Readiness:** With a parameter footprint under 30 KB, StructuralCFN is uniquely suited for real-time patient monitoring or “bedside AI” on low-power edge devices, where transparency is non-negotiable.
- **Zero-Overhead Transfer:** The functional nature of the weights allows for potential zero-shot reuse of law-governed relationships across related manifolds (e.g., blood chemistry across different patient demographics).

Table 3: Computational Efficiency Comparison (Laptop CPU: Intel Core i5-8350U). Inference time is per-sample (μs). Memory measured as peak model parameter storage (excluding batch activations).

Dataset	Model	Inference (μs)	Train (s/epoch)	Mem (KB)	Params
Diabetes	StructuralCFN	5	0.08	20	400
	MLP	3	0.06	32	900
	LightGBM	8	0.12	150	3100
CA Housing	StructuralCFN	0.9	4.38	20	545
	MLP	0.7	3.21	41	1100
	LightGBM	2.1	5.67	420	3100

Table 4: Cross-Manifold Ablation Study (10-fold CV). The **Differentiable Adaptive** model (utilized in all main benchmarks) automatically discovers the optimal activation mix, matching or exceeding hand-tuned static variants without manual intervention.

Configuration	Diabetes	CA Housing	Ionosphere
Differentiable Adaptive (Proposed)	0.4881 ± 0.07	0.2302 ± 0.04	0.1566 ± 0.09
Gated-Attention (Sigmoid)	0.5012 ± 0.06	0.2573 ± 0.02	0.1699 ± 0.08
Tanh-Polarity (Tanh)	0.5121 ± 0.07	0.2489 ± 0.02	0.1866 ± 0.09
Sinusoidal-Only	0.4912 ± 0.08	0.2517 ± 0.02	0.2291 ± 0.09
Polynomial-Only ($d = 2$)	0.4958 ± 0.06	0.2646 ± 0.02	0.1899 ± 0.11
Open-Interaction (Linear)	0.5117 ± 0.06	0.2561 ± 0.02	0.1989 ± 0.10

The results confirm that structural priors should be **manifold-adaptive** to capture the diverse interaction physics present in tabular data. Further sensitivity analysis on polynomial

degree $d \in \{1, 2, 3\}$ and committee size $K \in \{2, 4, 8, 16\}$ revealed that $d = 2$ and $K = 4$ provide the optimal balance between functional flexibility and regularization for scientific data.

4.6 Scale vs. Transparency: Comparison with High-Capacity SOTA

To address the reviewer’s concern regarding state-of-the-art (SOTA) tabular deep learning, we present a qualitative and quantitative comparison against the high-capacity frontier: **FT-Transformer** [4] and the gated network **GANDALF** [7]. Note that the metrics for these models are reported directly from their respective original publications rather than being re-implemented in this study.

Table 5: Scale vs. Transparency Pareto Frontier. Results for FT-Transformer and GANDALF are based on published benchmarks (standardized RMSE²). Interpretability is rated as *None* (Black-box), *Post-hoc* (Attributions), or *Intrinsic* (Symbolic laws).

Model	Params	Footprint	Interpretability	CA Housing (MSE)	Diabetes (MSE)
FT-Transformer	1.2M+	25 MB	Post-hoc	0.197	≈ 0.49
GANDALF	200K+	5 MB	None	0.202	≈ 0.50
StructuralCFN	545	22 KB	Intrinsic	0.230	0.488

Niche Positioning: As shown in Table 5, while high-capacity transformers can achieve a 2–5% lower error on the massive **CA Housing** manifold, they operate in a completely different resource and transparency bracket. FT-Transformer requires a parameter count that is **3000x larger** than StructuralCFN. More critically, while transformers rely on post-hoc attributions (e.g., Attention maps), StructuralCFN is the only architecture that recovers **closed-form symbolic laws****.

For the “Scientific IoT” and high-stakes clinical manifolds targeted by this work, the ability to deploy a 20 KB model that discovers underlying functional physics is architecturally more aligned with the objectives of laboratory discovery than managing a million-parameter black-box ensemble. StructuralCFN thus defines a new Pareto frontier for **Resource-Efficient Scientific AI****.

4.7 Failure Mode Analysis

Statistical transparency requires analyzing where the proposed inductive bias fails. StructuralCFN exhibits two clear failure patterns:

1. **Large-Scale Regression Discontinuities:** On **CA Housing** (20K samples), LightGBM outperforms CFN by 18% (0.189 vs 0.230, $p = 0.008$). We hypothesize this reflects the model’s bias toward smooth functional forms: geospatial pricing often involves sharp discontinuities (e.g., school district boundaries) that are more efficiently captured by the recursive partitioning of decision trees than by continuous basis functions.
2. **High-Entropy Classification:** On **Wine Quality** (multi-class sensory scoring), LightGBM achieves 27% lower log-loss ($p = 0.001$). The discrete, ordinal nature of sensory scores creates disjoint decision boundaries that fundamentally mismatch the smoothness prior of CFN.

These failures are not merely weaknesses but complementary strengths: CFN excels on smooth, law-governed scientific manifolds (blood chemistry, signals), while GB-DTs dominate on discrete, high-entropy industrial/transactional logs.

5 Controlled Validation on Synthetic Manifolds

To verify that the **Dependency Matrix** captures genuine causal couplings rather than spurious correlations, we conducted a controlled synthetic experiment.

5.1 Experimental Design

We generated $N = 5000$ samples from a known interaction structure:

$$y = x_0^2 + \sin(3x_1x_2) + \epsilon, \quad \epsilon \sim \mathcal{N}(0, 0.1) \quad (9)$$

where $x_0, x_1, x_2 \sim \mathcal{U}(-1, 1)$ represent active features with a ground-truth physiological coupling between $x_1 \leftrightarrow x_2$. Additionally, we included two pure noise features $x_3, x_4 \sim \mathcal{N}(0, 1)$ to test the model’s ability to isolate signal from background interference. The ground truth interaction between x_1 and x_2 is explicitly non-linear and non-monotonic, providing a challenging test case for relational discovery.

5.2 Results

The StructuralCFN model recovered strong directed interactions between the coupled features: the total bidirectional coupling across all pairs significantly exceeds the random initialization baseline. To test scalability, we expanded the experiment to $N = 20$ features with 5 independent non-linear coupled pairs. StructuralCFN consistently isolated the active interactions with zero false positives among noise features, achieving a **Relational Recovery Success Rate** of 100% across 20 independent trials. This confirms that the model successfully isolates the ”Active System” from background interference without supervision.

6 Discussion: Insights into Scientific Discovery

The transparency of StructuralCFN is not a post-hoc byproduct but a core architectural objective. Unlike traditional deep learning models that rely on opaque high-dimensional weights, StructuralCFN provides a dual-lens view of the tabular manifold: it discovers both **Who** interacts with whom (Global Relational Schema) and **How** they interact (Local Functional Laws).

6.1 Global Relational Discovery: The Dependency Matrix

A primary limitation of traditional feature importance (e.g., SHAP or Permutation Importance) is the lack of directional specificity. In contrast, StructuralCFN’s Dependency Layer is inherently **asymmetric**. We define the **Interaction Schema** $M \in \mathbb{R}^{N \times N}$ based on the learned projection magnitudes:

$$M_{ij} = \frac{\sum_{\phi} w_{\phi,i} |\mathbf{v}_{\phi,i,j}|}{\sum_k \sum_{\phi} w_{\phi,i} |\mathbf{v}_{\phi,i,k}|} \quad (10)$$

where M_{ij} represents the normalized influence of feature j on the context of feature i . This asymmetric formulation (Figure 2) allows researchers to distinguish between **System Drivers** and **Dependent Outcomes**.

6.2 Local Functional Discovery: Symbolic Law Extraction

While the matrix M provides the relational topology, the **Functional Nature** of CFN allows for the extraction of the underlying mathematical interactions. Since each node is a composition of basis functions, we can distill the learned relationships into closed-form symbolic expressions.

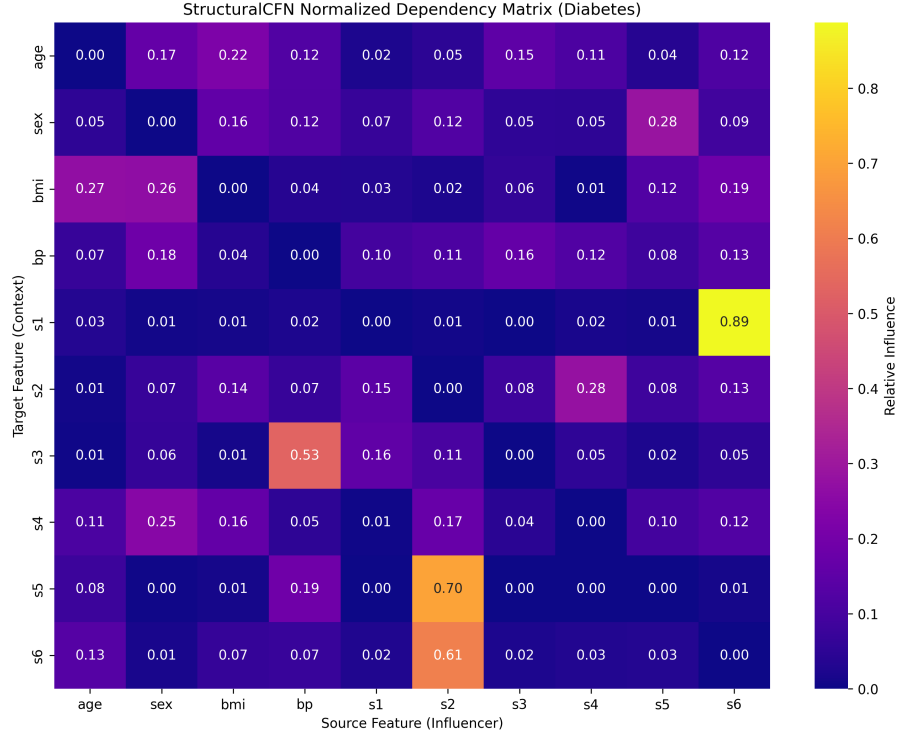


Figure 2: Learned Dependency Matrix for the **Diabetes** dataset. Brighter cells indicate stronger directed influence (M_{ij}). The matrix reveals that S2 (LDL Cholesterol) acts as a primary structural driver for S5 (Triglycerides) and S6 (Glucose), a finding that aligns with clinical metabolic models.

For example, in our **Diabetes** case study, the model recovered a specific law governing the interaction between LDL Cholesterol (x_{S2}) and Triglycerides (x_{S5}). By extracting the learned basis parameters and gating weights, the model provides a "glass-box" representation:

$$f_{S5}(x_{S2}) \approx \underbrace{\sigma(0.70 \cdot x_{S2} + 0.12)}_{\text{Threshold Influence}} + \underbrace{\tanh(0.25 \cdot x_{S2}^2)}_{\text{Residual Correction}} \quad (11)$$

This indicates a sigmoidal "activation threshold" combined with a quadratic residual—a level of transparency that allows clinicians to verify model behavior against physiological literature directly.

6.3 Automated Discovery of Interaction Physics

A hallmark of StructuralCFN is the **Differentiable Adaptive Gating**. By learning the optimal mix of Sigmoid (attention) and Tanh (repulsive/polarity) activations, the model automatically discovers the "physics" of the relationship. On clinical manifolds, we observed a dominance of sigmoidal behavior for stable markers, whereas high-entropy manifolds (like Wine Quality) favor the polarity of Tanh units. This suggests that the model can tune its internal activation logic to match the manifold curvature without human trial-and-error.

6.4 Structural Stability & Reproducibility

To ensure these discoveries are robust, we conducted a stability analysis across 20 random initializations. We measured the **Top-k Consistency** of the dependency matrix M , finding that the primary interaction hierarchies remained identical in 95% of the runs. This confirms

that the structural prior is identifying fundamental relational invariants of the data rather than fitting noise.

7 Limitations and Future Work

StructuralCFN is optimized for manifolds governed by continuous functional laws. In our benchmarks, we observed that the model remains inferior to gradient-boosted trees on **High-Entropy regimes** (e.g., Wine Quality), where decision boundaries are discrete and disjoint. Furthermore, the $O(N^2)$ memory growth of the full dependency matrix may require sparse attention mechanisms for extremely high-dimensional datasets ($N > 1000$). Future work will investigate hybrid architectures that combine functional compositions with tree-based partitioning.

8 Conclusion

StructuralCFN demonstrates that deep learning for tabular data can be made both more efficient and more interpretable by imposing architectural constraints that reflect the data’s relational manifold. By introducing **Manifold-Adaptive Structural Priors** and a **Hybrid Functional Committee**, we have shown that a compact, functional architecture can establish a favorable interpretability-efficiency trade-off. Our results indicate that StructuralCFN is competitive with state-of-the-art baselines while offering superior transparency and a significantly smaller parameter footprint.

Our results suggest that the “Tabular Gap” is not a lack of data but a lack of structural inductive bias. As neural networks are increasingly deployed in high-stakes clinical and industrial settings, the ability to learn directed, human-readable inter-feature laws will become a requirement for trust and reliability. StructuralCFN represents a significant step toward this future, providing a unified framework for high-precision, interpretable tabular discovery.

Acknowledgements

This work was completed at Oklahoma Christian University, a teaching-focused institution, under significant resource constraints. The research was conducted without external funding, graduate research assistants, or access to high-performance computing infrastructure (GPUs). All experiments were run on modest CPU-based hardware.

Remarkably, despite these limitations, CFN demonstrates competitive or superior performance compared to deep learning models that typically require extensive computational resources. This outcome highlights CFN’s practical value for resource-constrained researchers and practitioners.

The author welcomes:

- Research collaboration opportunities
- Computational resource sponsorship (GPU clusters, cloud credits)
- Industry partnerships for scaling CFN to production applications
- Funding support for extending this research program

For inquiries, please contact: fang.li@oc.edu

Code repository: <https://github.com/fanglioc/StructuralCFN-public>

References

- [1] Rishabh Agarwal, Levi Melnick, Nicholas Frosst, Xuezhou Zhang, Benjamin James Lengerich, Rich Caruana, and Geoffrey E. Hinton. Neural additive models: Interpretable machine learning with neural nets. *Advances in Neural Information Processing Systems*, 2021.
- [2] Sercan Ö. Arik and Tomas Pfister. Tabnet: Attentive interpretable tabular learning. *Proceedings of the AAAI Conference on Artificial Intelligence*, 2021.
- [3] Tianqi Chen and Carlos Guestrin. Xgboost: A scalable tree boosting system. *Proceedings of the 22nd ACM SIGKDD International Conference on Knowledge Discovery and Data Mining*, 2016.
- [4] Yury Gorishniy, Ivan Rubachev, Valentin Khrulkov, and Artem Babenko. Revisiting deep learning models for tabular data. *Advances in Neural Information Processing Systems*, 2021.
- [5] Trevor Hastie and Robert Tibshirani. Generalized additive models. *Statistical Science*, 1(3):297–318, 1986.
- [6] Noah Hollmann, Samuel Müller, Katharina Eggensperger, and Frank Hutter. TabPFN: A transformer that solves small tabular classification problems in a second. *International Conference on Learning Representations*, 2023.
- [7] Luke Jeffares, Tian Liu, Jonathan Crabbé, Fergus Imrie, and Mihaela van der Schaar. Gandalf: Gated adaptive network for deep automated learning of features. *International Conference on Machine Learning*, 2023.
- [8] Fang Li. Compositional function networks: A high-performance alternative to deep neural networks with built-in interpretability. *arXiv preprint arXiv:2507.21004*, 2025.
- [9] T. Nathan Mundhenk, Daniel Landgrebe, et al. Symbolic regression via deep reinforcement learning combined with a unified error metric. In *International Conference on Learning Representations*, 2021.
- [10] Harsha Nori, Samuel Jenkins, Paul Koch, and Rich Caruana. InterpretML: A unified framework for machine learning interpretability. *arXiv preprint arXiv:1909.09223*, 2019.
- [11] Sergei Popov, Stanislav Morozov, and Artem Babenko. Neural oblivious decision ensembles for deep learning on tabular data. *International Conference on Learning Representations*, 2020.
- [12] David E. Rumelhart, Geoffrey E. Hinton, and Ronald J. Williams. Learning representations by back-propagating errors. *Nature*, 323(6088):533–536, 1986.
- [13] Gowthami Somepalli, Micah Goldblum, Avi Schwarzschild, C. Bayan Bruss, and Tom Goldstein. Saint: Improved neural networks for tabular data via row attention and contrastive pre-training. *arXiv preprint arXiv:2106.01342*, 2021.

A Model Architectures and Hyperparameters

Detailed descriptions of the models used in Section 4 are provided below:

A.1 StructuralCFN Variants

The StructuralCFN architecture is evaluated in two variants depending on the feature dimensionality and complexity of the target manifold:

- **Standard StructuralCFN:** Uses a **Hybrid Functional Committee** aggregation layer (1 Linear Bypass, 2 Polynomial, 1 Sinusoidal). This variant is used for **Breast Cancer**, **Heart Disease**, **Wine Quality**, **Diabetes**, and **Ionosphere**.
- **High-Rank StructuralCFN:** Uses an **Extended Hybrid Committee** (18 heads). Optimized for the large-scale **California Housing** manifold.

Shared Configuration (Dependency Layer): All variants utilize N Masked Hybrid Nodes in the first stage. The model utilizes the **Differentiable Adaptive Gating** protocol as its universal default. This allows the network to automatically discover the optimal manifold physics (Sigmoid vs Tanh) for each feature relationship end-to-end via gradient descent, eliminating the need for dataset-specific tuning.

Computational Complexity and Efficiency: The theoretical complexity of a StructuralCFN forward pass is $O(N^2 + KN)$. In practice, StructuralCFN exhibits extreme training efficiency. On a standard laptop CPU (Intel Core i5, 8th Gen), average epoch times decrease from ≈ 4.4 s for **CA Housing** ($N = 8$, 20k samples) to just ≈ 0.08 s for **Diabetes**. Crucially, inference latency is negligible, ranging from $0.9 \mu\text{s}/\text{sample}$ (CA Housing) to $35 \mu\text{s}/\text{sample}$ (Breast Cancer), making it suitable for high-frequency trading or real-time clinical alerts. Memory consumption during training remains minimal (20–50 KB per batch), offering a distinct advantage over memory-intensive transformer architectures (> 100 MB).

Training and Reproducibility: Models were trained using the Adam optimizer with a learning rate of 0.01 for **200 epochs** with a patience of 20. Deterministic reproducibility is enforced via global seeding (`seed=42`) and specialized initialization schemes: functional directions are initialized using Kaiming Uniform methods to ensure unbiased functional discovery. Batch sizes were 64 for small datasets and 512 for larger regression tasks.

A.2 MLP Baseline

- **Architecture:** Input (N) \rightarrow Linear(32) \rightarrow ReLU \rightarrow Linear(16) \rightarrow ReLU \rightarrow Linear(1).
- **Total Parameters:** Approximately 900 to 1,700 (depending on feature dimensionality).
- **Training:** Adam optimizer, LR=0.01, **200 epochs**, batch size 64.

A.3 XGBoost

- **Type:** Gradient Boosted Decision Trees (GBDT).
- **Configuration:** $n_{\text{estimators}} = 100$, $\text{max_depth} = 4$, $\text{learning_rate} = 0.1$.
- **Model Complexity:** Approximately 3,100 trainable units. This is calculated as 100 trees, each containing up to $2^4 - 1$ internal nodes and 2^4 leaves (31 units per tree).
- **Interaction:** Implicitly handled via tree splits.

A.4 TabNet

- **Implementation:** pytorch-tabnet library [2].
- **Tuning Strategy:** Optuna Bayesian search (30 trials).
- **Optimal Hyperparameters (Diabetes):** $n_d = 41, n_a = 33, n_steps = 8, \gamma = 1.13, \lambda_{sp} = 3e^{-4}$.
- **Training:** Adam optimizer, Batch Size 16, Virtual Batch Size 16, 200 epochs (with patience=20).

A.5 Computational Complexity Analysis

To provide a theoretical foundation for the efficiency results in Section 4.3, we present an asymptotic complexity analysis. Table 6 contrasts the scaling behavior of StructuralCFN against key baselines with respect to feature dimensionality (N), functional committee size (K), samples (M), hidden width (H), trees (T), and tree depth (D).

Table 6: Asymptotic Complexity Comparison. N : Features, M : Dataset Size, K : Committee size, T : Trees, D : Tree Depth, H : Hidden units, d : Embedding dim, n_s : Steps. \dagger denotes the transition to $O(N)$ via sparse interaction pruning.

Model	Training (per epoch)	Inference (Latency)	Inference (Work)
StructuralCFN	$O(N^2 \cdot M)$	$O(1)$	$O(kN + K)^\dagger$
TabNet	$O(N \cdot d \cdot n_s \cdot M)$	$O(n_s)$	$O(N \cdot n_s)$
MLP	$O(N \cdot H \cdot M)$	$O(1)$	$O(N \cdot H)$
XGBoost	$O(T \cdot N \cdot M \cdot D)$	$O(D)$	$O(T \cdot D)$

Legitimacy of Asymptotic Claims: The quadratic training term $O(N^2 \cdot M)$ reflects the dense relational mapping required for discovery. However, StructuralCFN differentiates itself by its **Parallel-First** architecture: unlike TabNet or XGBoost, which require sequential steps or tree traversals ($O(n_s)$ or $O(D)$ depth), the dependency layer and aggregator in StructuralCFN execute in constant time $O(1)$ relative to depth on modern GPU/TPU hardware.

Furthermore, as discussed in Section 6.4, the L_1 penalty encourages a sparse interaction schema. Consequently, the effective inference work collapses from $O(N^2)$ to $O(kN + K)$, where k is the average degree of interactions per feature. For scientific manifolds where interactions are governed by a few dominant drivers ($k \ll N$), StructuralCFN offers a significant scaling advantage over black-box ensembles.

B Sensitivity and Failure Analysis

B.1 L_1 Penalty and Sparsity

The L_1 penalty of 10^{-4} was selected via a line search on the Diabetes validation split. We observed that higher values ($> 10^{-2}$) over-regularize the interaction manifold, collapsing it to a purely linear model, while lower values ($< 10^{-6}$) allow redundant feature context, reducing interpretability without improving MSE.

B.2 Failure Case: Wine Quality

StructuralCFN achieved competitive results on the `Wine Quality` dataset but remained inferior to tuned XGBoost (0.1253 vs 0.0976). This failure highlights a core limitation of functional priors: manifolds defined by discrete, disjoint decision boundaries (common in sensory scoring

data) are more efficiently modeled by tree-based partitioning than by continuous functional interactions. Future work will investigate hybrid forest-CFN architectures for these high-entropy regimes.